DTIC COPY

REPORT DOCUMENTATION PAGE

Form Approved
OMB No. 0704-01-0188

PLEASE DO NOT RETURN YOUR FORM TO THE ABOVE ADDRESS.

1. REPORT DATE *(DD-MM-YYYY)*	2. REPORT TYPE	3. DATES COVERED *(From - To)*
03-12-2007	REPRINT	

4. TITLE AND SUBTITLE

Proton Flux Anisotropy in Low Earth Orbit

5a. CONTRACT NUMBER

5b. GRANT NUMBER

5c. PROGRAM ELEMENT NUMBER
62601F

6. AUTHORS
Gregory P. Ginet
Bronislaw K. Dichter*
Donald H. Brautigam
Dan Madden**

5d. PROJECT NUMBER
1010

5e. TASK NUMBER
RS

5f. WORK UNIT NUMBER
A1

7. PERFORMING ORGANIZATION NAME(S) AND ADDRESS(ES)

Air Force Research Laboratory /RVBXR
29 Randolph Road
Hanscom AFB, MA 01731-3010

8. PERFORMING ORGANIZATION REPORT NUMBER
AFRL-RV-HA-TR-2008-1015

9. SPONSORING/MONITORING AGENCY NAME(S) AND ADDRESS(ES)

10. SPONSOR/MONITOR'S ACRONYM(S)
AFRL/RVBXR

11. SPONSOR/MONITOR'S REPORT NUMBER(S)

12. DISTRIBUTION/AVAILABILITY STATEMENT
Approved for Public Release; distribution unlimited.

13. SUPPLEMENTARY NOTES
Reprinted from *IEEE Transactions on Nuclear Science*, Vol. 54, No. 6, December 2007 © 2007 IEEE.

14. ABSTRACT

Proton flux anisotropy as a function of altitude in the South Atlantic Anomaly (SAA) is investigated using data from the Compact Environment Sensor (CEASE) flown onboard the Tri-Service Experiment-5 (TSX-5) satellite from June 2000 to July 2006. In a 410 x 1710 km, 69 degree inclination orbit, TSX-5 spanned a broad range of the low Earth orbit regime. Using measurements of total dose, integral energy flux >40 MeV and the differential flux at 40 MeV sorted into 3 degree latitude x 3 degree longitude x 50 km altitude bins and averaged over the entire misison, the components arising from eastward and westward traveling protons have been determined in areas of the SAA where CEASE detection efficiency is not compromised. For the first time, ratios of these components have been compared to predictions of East-West effect models above 400 km. There is good agreement in general with the anisotropy becoming apparent at approximately 1200 km (moving down) and increasing rapidly starting at approximately 1000 km, the magnitude and rate depending on location within the anomaly. Measurement of the differential flux at 40 MeV are compared to predictions of standard radiation belt models as a function of altitude and found to be substantially higher in magnitude than AP8, though a comprehensive survey has not yet been performed.

15. SUBJECT TERMS
Radiation belts Radiation effects South Atlantic Anomaly

16. SECURITY CLASSIFICATION OF:			17. LIMITATION OF ABSTRACT	18. NUMBER OF PAGES	19a. NAME OF RESPONSIBLE PERSON
a. REPORT	b. ABSTRACT	c. THIS PAGE			Gregory P. Ginet
UNCL	UNCL	UNCL	Unl	8	19B. TELEPHONE NUMBER *(Include area code)*

Proton Flux Anisotropy in Low Earth Orbit

Gregory P. Ginet, Bronislaw K. Dichter, Donald H. Brautigam, and Dan Madden

***Abstract*—Proton flux anisotropy as a function of altitude in the South Atlantic Anomaly is investigated using data from the Compact Environment Anomaly Sensor (CEASE) flown onboard the Tri-Service Experiment-5 (TSX-5) satellite from June 2000 to July 2006. In a 410 km × 1710 km, 69 degree inclination orbit, TSX-5 spanned a broad range of the low Earth orbit regime. Using measurements of total dose, integral energy flux >40 MeV and the differential flux at 40 MeV sorted into 3 degree latitude × 3 degree longitude × 50 km altitide bins and averaged over the entire mission, the components arising from eastward and westward traveling protons have been determined in areas of the SAA where CEASE detection efficiency is not compromised. For the first time, ratios of these components have been compared to predictions of East-West effect models above 400 km. There is good agreement in general with the anisotropy becoming apparent at approximately 1200 km (moving down) and increasing rapidly starting at approximately 1000 km, the magnitude and rate depending on location within the anomaly. Measurements of the differential flux at 40 MeV are compared to predictions of standard radiation belt models as a function of altitude and found to be substantially higher in magnitude than AP8, though a comprehensive survey has not yet been performed.**

***Index Terms*—Radiation belts, radiation effects, South Atlantic anomaly.**

I. Introduction

At altitudes below approximately 1000 km the trapped proton flux in the inner Van Allen radiation belt is strongly influenced by the neutral atmosphere, while above that altitude magnetic field effects dominate. The atmospheric influence can create an anisotropy in proton fluxes at low altitudes resulting in eastward proton fluxes being greater than the westward ones. This "East-West" (EW) effect was first proposed by Lenchek and Singer [1] in 1962, and measurements of the effect were first reported in 1963 by Heckman and Nakano [2].

As a consequence of the anisotropic flux distribution radiation doses received by components in various locations on a three axes stabilized spacecraft can vary significantly. Identical electrical, electronic and electromechanical (EEE) parts located behind the same amount of shielding material will experience different radiation doses and single event effect environments.

Manuscript received July 21, 2007; revised October 5, 2007.

G. P. Ginet and D. H. Brautigam are with the Space Vehicles Directorate, Air Force Research Laboratory, Hanscom AFB, MA 01731 USA (e-mail: afrl.rvb.pa@hanscom.af.mil).

B. K. Dicther was with the Space Vehicles Directorate, Air Force Research Laboratory, Hanscom AFB, MA 01731 USA. He is now with Assurance Technology Corporation, Carlisle, MA 01741 USA (e-mail: dichter@assurtech.com).

D. Madden is with the Institute for Scientific Research, Boston College, Boston, MA 02467 USA (e-mail: afrl.rvb.pa@hanscom.af.mil).

Color versions of one or more of the figures in this paper are available online at http://ieeexplore.ieee.org.

Digital Object Identifier 10.1109/TNS.2007.910041

Measurements of the EW effect so far reported have been confined to the lower portion of the low Earth orbit (LEO) regime between ~250–400 km [2]–[6]. In this paper we present the first study of the EW dose and proton flux anisotropies over the range of altitudes from 400–1700 km. Data in the epoch 2000–2006 from the Compact Environment Anomaly Sensor (CEASE) onboard the Tri-Service Experiment-5 (TSX-5) satellite is utilized. Section II reviews the theory and modeling work which has been done on the EW effect. CEASE data analysis methods are described in Section III and the comparison of data to theory is presented in Section IV. The paper is summarized in Section V.

II. Models of the East-West Effect

Protons moving eastward at the location of a satellite have their centers of gyration above the satellite, while the westward moving ones have them below. In a regime where the neutral density is changing relatively rapidly, i.e. with a scale height on the order of the gyroradius, and of a magnitude where it affects the motion of trapped protons through ionization energy loss and nuclear scattering, the particles moving westward will have experienced more neutral density interactions than those traveling eastward. At a fixed energy and pitch-angle, fluxes measured by a westward pointing instrument should therefore be larger than those of a eastward pointing instrument.

Consider a coordinate system with origin at an observation point in near-Earth space and the z axis aligned with the local magnetic field ($\mathbf{B}$) direction. The y axis points toward the magnetic east in the direction $\mathbf{B} \times \mathbf{R}$, where $\mathbf{R}$ is the vector from the center of the Earth to the point, and the $x - y$ plane is the local magnetic mirror plane with $x = y \times z$ pointing magnetically "upwards". Let $\mathbf{j}$ be a differential particle flux vector expressed in the $x - y - z$ system and the corresponding spherical coordinate system angles θ and φ represent the pitch angle and east-west angle, respectively, such that $0 < \varphi < \pi$ ($\pi < \varphi < 2\pi$) means $\mathbf{j}$ points east (west). Assuming that the magnitude of the particle flux at the observation point is inversely proportional to the neutral density at the guiding center of the particle, and that the density varies exponentially with a scale height H, then the ratio of the magnitude of fluxes traveling in directions 1 and 2 as observed at the origin is

$$\frac{j_1}{j_2} = \exp\left\{\frac{a}{H}\cos I(\sin\theta_1 \sin\varphi_1 - \sin\theta_2 \sin\varphi_2)\right\} \quad (1)$$

where a is the particle gyroradius and I is the magnetic inclination (angle between $\mathbf{B}$ and the geographic horizontal plane measured positive downwards). For particles in the mirror plane with j_1 (j_2) due east (west) the exponent reaches the maximum value of $2a\cos I/H$, as originally derived by Lencheck and Singer.

Further progress can be made by including details of the particle pitch angle distribution. Gaussian and more complex distributions, all with the common property of being sharply peaked about the local mirror plane angle, have been analyzed. Watts *et al.* [7] have combined the Lenchek and Singer anisotropy function ((1)), the Heckman and Nakano Gaussian pitch angle distribution [3] and the omnidirectional fluxes predicted by the NASA AP8 model [8] to produce a model of the anisotropic flux distribution. Armstrong *et al.* [9] have integrated the Watts *et al.* model into a dose prediction tool targeted to space station altitudes. Kruglanski [10] has produced a tool of the same nature using the more complex Badhwar and Konradi pitch angle distribution [11]. Both the Armstrong *et al.* and Kruglanski applications are available on the SPENVIS website (http://www.spenvis.oma.be/spenvis/). It should be noted that these models have been parameterized to apply to satellites in orbit at altitudes of less than approximately 600 km.

III. Analysis Methods

The TSX-5 spacecraft was launched on June 7, 2000 into a 410 × 1710 km, 69 degree inclination orbit and the CEASE instrument collected data for the entire mission until termination on July 5, 2006. CEASE is comprised of two dosimeters and a particle telescope. The telescope consists of two coaxial Si solid-state detectors that measure the energy deposited in them by incident particles.

A. Instrument Characterization

Specifications and methods for optimizing the environmental information obtained from CEASE are described in detail elsewhere [12]–[14] and will be briefly summarized here as they pertain to protons. The response of the dosimeters and telescope to incident protons was extensively modeled using the Monte Carlo MCNPX computer code which simulates the passage of particles through material. Detector responses were determined for protons with energies between 20 and 200 MeV and for angles of incidence up to 90 degrees from the center axis corresponding to the detector look direction. Fig. 1 shows several typical simulation results in the form of effective area as a function of angle. In general, detection efficiency drops substantially beyond ~30 degrees (~0.25 max value at 30 deg) thus establishing an effective symmetric field of view angle of ~60 degrees centered on the look direction. Proton beam calibrations of the instruments to validate the computer modeled response are planned for another identical CEASE flight unit but have not yet been performed. However, comparisons of the Monte Carlo derived results for the angular response of the telescope have been compared to results of a simple analytical model of a two element telescope. The agreement between the two different calculations is very good.

For this study three specific CEASE outputs are used:

1) Total Dose: The total dose was determined by summing the responses of the three linear energy transfer (LET) channels in the dosimeter situated behind 250 mils of aluminum.

2) Integral Energy Flux >40 MeV: An approximation to the integral energy flux above 40 MeV is determined by applying an appropriate geometric factor to one of the dosimeter LET channels (D06). The geometric factor and threshold energy

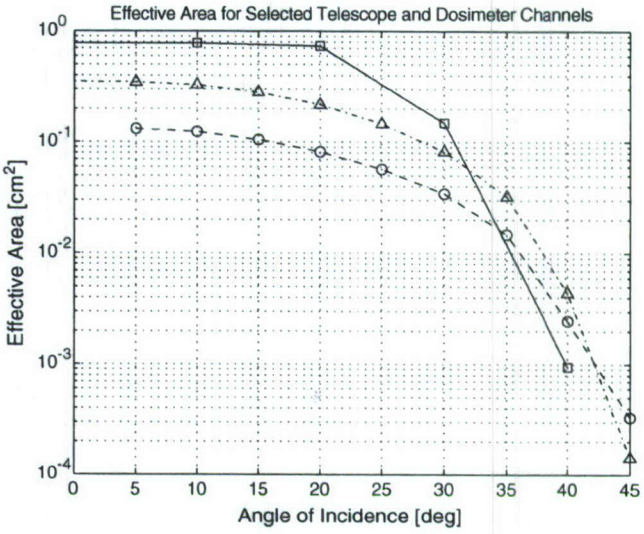

Fig. 1. Effective area as a function of angle of incidence resulting from Monte Carlo simulations of CEASE dosimeter channel D06 (square) and telescope channels T06 (circle) and T08 (triangle) with sensitivity to protons of approximately >40 MeV, >40 MeV, and >94 MeV, respectively.

were obtained by assuming that dosimeter channel energy-dependent response function approximates a step function, where the step occurs at the threshold energy E_T, and then demanding that that the integral flux for energy > E_T calculated by integrating the response function with an estimated isotropic power law flux distribution is equivalent to the quotient of the channel count rate divided by the geometric factor. Though the geometric factor drops out when comparing ratios of fluxes, the procedure was necessary to estimate the threshold energy and also provided a useful check on the differential flux estimating procedure as described below.

3) Differential Flux at ~40 MeV: A spectral inversion algorithm utilizing the count rates from one dosimeter and 5 telescope channels was employed to estimate the differential flux spectrum. The count rate for each channel is related to the channel response function and the differential flux j through an integral equation. Assuming an isotropic power law distribution for the flux, the scheme iteratively determines a unique pair of amplitude and exponent that minimizes the variation of power law amplitude needed to match the observed count rates across all channels. An estimate of the uncertainty then comes directly from the magnitude of the minimized amplitude variation.

B. Geophysical Domain

Count rate measurements in 5 s intervals from all CEASE channels for the entire mission were binned into a database separated into geographical cells; 3 degrees × 3 degrees in longitude and latitude and 50 km in altitude over the range 400–1650 km. To maintain focus on the properties of the trapped proton distributions all data from time intervals comprising solar proton events (SPEs) were removed. A SPE was defined as the time interval when the Space Environment Monitor (SEM) detector's >10 MeV proton channel on the GOES geosynchronous satellite measured greater than 10 protons/(cm^2 sec str). After SPE removal there were typically greater than 100 measurements per bin. A background count rate for each channel and altitude was

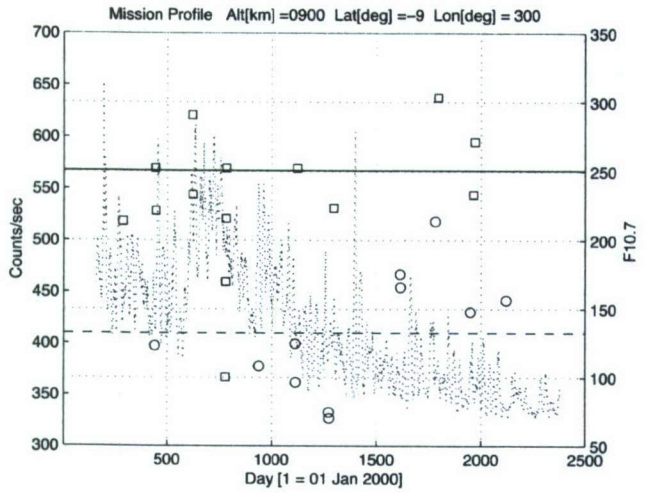

Fig. 2. Counts per second in the D06 dosimeter channel for passes through the 900 km, −9 deg latitude and 300 deg longitude bin as a function of mission time for the two different look angles (circles and squares) characteristic of the bin. The solid (dashed) line is the median value of the westward (eastward) *looking* angle. Daily averaged F10.7 flux (dotted line) shows solar activity during the course of the mission.

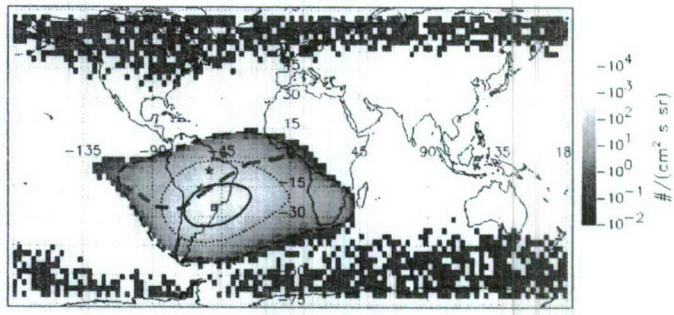

Fig. 3. Map of the SAA at 800 km derived from the T06 telescope channel (>40 MeV) showing contour boundaries for maximum (square), 1/2 maximum (solid line), 1/10 maximum (dotted line) and 3 sigma times background (dashed line) levels. The thick dashed line gives the southern boundary of the region analyzed in this work. Stars indicate the points used in Figs. 4–6.

determined by performing a Poisson fit to the distribution of count rates at intermediate latitudes outside of the anomaly but below latitudes where the telescope becomes sensitive to high energy electrons in the horns of the outer belt. The background was subsequently subtracted from the channel data. Finally, the sequence of measurements from each single pass through a bin (typically TSX-5 will have a sequence of several 5 s intervals when going through a bin) was averaged to obtain a reduced set of pass-averaged measurements.

Fig. 2 illustrates a typical distribution of the pass-averaged count rate measurements in the SAA over the entire mission. In this particular case it is data from the D06 channel for a bin at −9 degree latitude, 300 degree longitude and 900 km in altitude. A double peak distribution in amplitude is apparent and was found to be correlated with the look direction of the CEASE detector. On north-to-south passages the look direction had a westward component (squares) measuring eastward traveling particles while on south-to-north passages the look direction had an eastward component (circles). The solid (dashed) line is the mean of the west (east) looking measurements. Variations in the look direction with respect to the local magnetic field have variations of less than 5 degrees for either the south or north bound cluster for the entire mission data set indicating that comparisons of mission average quantities might yield statistically significant results. Also shown in Fig. 2 is the daily F10.7 radio flux (dotted line), an indicator of solar activity and a cause of neutral atmospheric variation. In the first half of the mission conditions were characteristic of solar maximum whereas the second half captures the decay into solar minimum.

Our analysis is confined to a portion of SAA as mapped out in Fig. 3 at the altitude of 800 km. The SAAMAP was constructed from TSX5/CEASE telescope data and is reported elsewhere [15]. Closed boundaries representing 1/2 the maximum flux (solid), 1/10 the maximum flux (dotted) and 3 times the background count rate (dashed) are shown as is the point of maximum flux (square). A thick dashed line across the middle of the anomaly bounds on the south the region of our analysis (containing three stars) with a boundary on the north defined by the 1/10 max contour. Obviously the lack of particles to measure is a good reason for the northern boundary. The reason for imposing the southern boundary lies in the CEASE angular response, the particle pitch angle distributions sharply peaked near 90 degrees, and the relative angle between the CEASE look direction and the local magnetic field as determined by the spacecraft orbit. Below this boundary the CEASE look angle is more than 30 degrees away from the local mirror plane thereby leading to significant decrease in CEASE counting efficiency (Fig. 1) and a consequent increase in uncertainty in the geometric factor and spectral fit algorithms employed. Since the detector response has been extensively modeled it is possible to develop more complex algorithms to correct for this situation at least to the degree of uncertainty in the pitch angle distribution. Such an effort is underway but will not be reported on here. Three specific points (the stars in Fig. 3) have been selected to illustrate the EW effect as a function of altitude.

IV. Results

A. *East-West Effect*

The directional effect observed by TSX5/CEASE was determined for the three separate quantities discussed in Section II for each bin by computing the mission average values for each of the two look directions characteristic of the bin and then taking the ratio. These ratios are shown in Fig. 4 as a function of altitude for the stack of bins at −18 degrees latitude, 300 degrees longitude for total dose (circle), integral energy flux (square) and differential energy flux (triangle). A nearest-neighbor smoothing function was applied to the points to remove jitter at the lower altitudes where the counting rates start to decrease. In this figure "East" (West) implies eastward (westward) traveling protons. That the ratio is consistent among all three empirical quantities derived using different components of the CEASE instrument gives confidence that a real effect is being observed. Similar consistency can be seen in the ratio profiles at −9 degrees latitude, 309 degrees longitude (Fig. 5) and 0 degrees latitude, 315 degrees longitude (Fig. 6). No empirical ratios are shown below

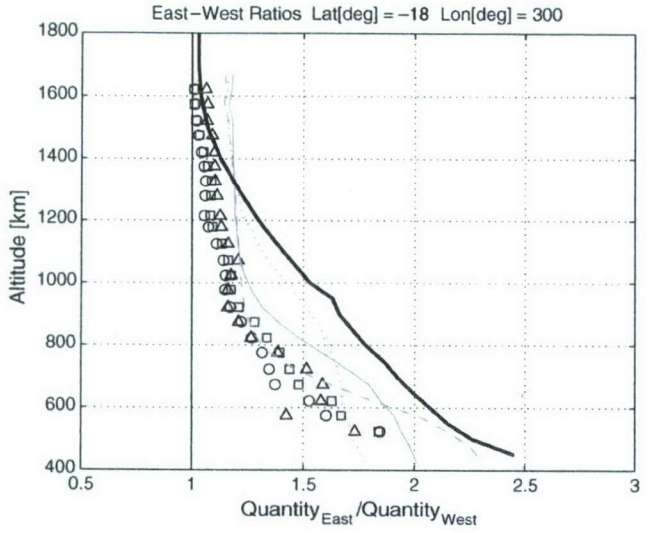

Fig. 4. Eastward/Westward traveling ratios for total dose (circle), integral energy flux >40 MeV (square), and differential energy flux at 40 MeV (triangle) as a function of altitude for the −18 deg latitude, 300 deg longitude bin. Model predictions are shown from Lencheck and Singer with density scale heights corresponding to an exoatmospheric temperature of 1000 K (solid), 800 K (dashed), and 1300 K (dotted). Maximum anisotropy factors from the SPENVIS version of the Watts et al. model are shown as the thick solid curve.

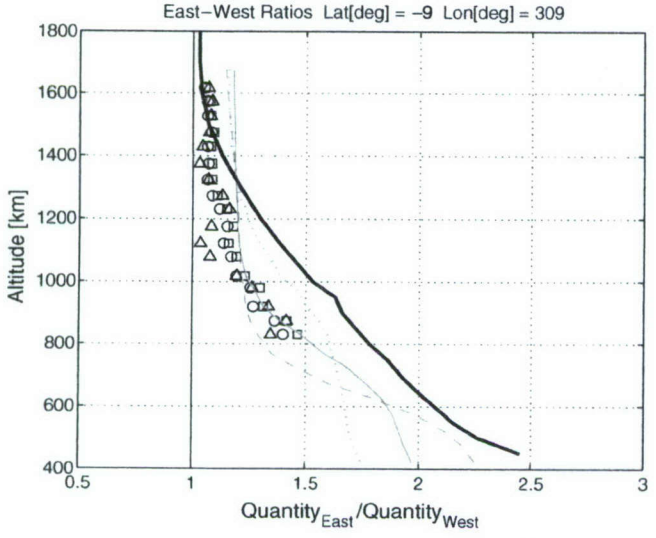

Fig. 5. Same as Fig. 4 for the −9 deg latitude, 309 deg longitude bin.

700 km (850 km) in Fig. 5 (Fig. 6) since they define the lower boundary of the anomaly at those latitude and longitudes [15].

Predictions of the EW ratio from the Lencheck & Singer model were made by computing the angles in (1) from averages corresponding to the two characteristic look directions of each bin. A height dependent gyroradius was calculated using the average magnetic field strength in each bin and assuming a 40 MeV particle. Altitude dependent density scale heights were taken from the Jacchia 1977 neutral density model [16]. The solid, dashed and dotted lines in Figs. 4, 5 are the model East-West differential flux ratios ((1)) for density scale heights profiles representing an exoatmospheric temperature of 1000 K, 800 K and 1300 K, respectively, corresponding to solar average, solar quiet, and solar active conditions. Our intent is not to match

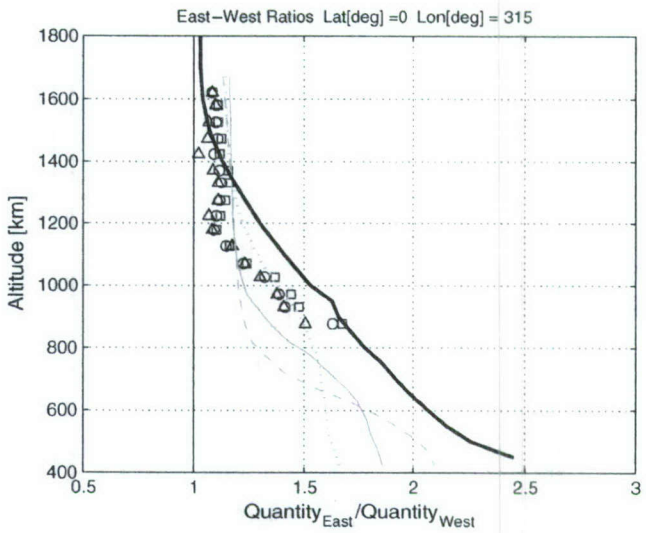

Fig. 6. Same as Fig. 4 for the 0 deg latitude, 315 deg longitude bin.

specific data to specific solar conditions but rather to show the degree of variability in the theoretical predictions of the EW ratio given the broad range of solar activity occurring during the TSX5 mission (Fig. 2).

A calculation of the modeled East-West ratios was also carried out using the SPENVIS anisotropy tool running the anisotropy model of Watts *et al.* [7]. In order to obtain an estimate of the East-West ratio as a function of altitude for the TSX-5 orbit we approximated the altitude effect by computing the ratios for a series of circular orbits with the same inclination as the TSX-5 orbit. Each such constant altitude orbit traverses nearly the same trajectories through the SAA as the TSX-5 spacecraft did at that altitude. The output of the calculations is a surface which is a function of polar and an azimuthal angle, where the polar axis is the spacecraft pointing vector. Projecting the surface onto the polar angle axis results in a curve with a maximum at 90 degrees and minima at 0 degrees and 180 degrees. This is what is expected of a polar angle lying predominantly along the north-south axis, since in that case the minimum flux would be traveling parallel to the magnetic field direction and the maximum in the plane normal to it. The projection of the surface on the azimuthal axis results in curve whose maximum is identified with the eastward moving proton flux and the minimum with the westward one. The resulting East-West ratios, as a function of the altitude of the circular orbits, are shown as the thick solid lines in Figs. 4–6. It should be emphasized that this is an upper bound to the empirical ratio since the CEASE look angles were not facing due east or due west in the mirror plane.

It is clear that the CEASE observations compare favorably to the model predictions. The EW effect is apparent, beginning at approximately 1200 km going down in altitude with rate of change increasing substantially below approximately 1000 km. Empirical ratios are close to the Lencheck and Singer predictions when variation due to solar activity are taken into account and nearly always less then the upper bound predicted by the SPENVIS tool except at the highest altitudes where the assumption of scaling of flux magnitude as the inverse of the density

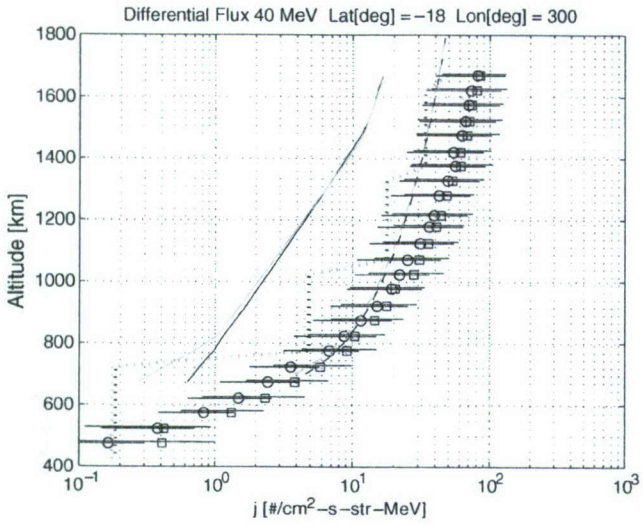

Fig. 7. Differential flux at 40 MeV verses altitude for CEASE measurements of eastward (square) and westward (circle) traveling fluxes. Model predictions are shown from AP8 for min (dark solid) and max (light solid), from CRRESPRO for quiet (dark dotted) and active (light dotted), and from TPM-1 for F10.7 = 95 (dark dashed) and 173 (light dashed). For a given model the dark curves have the larger flux values at lower altitudes.

breaks down. The profiles in Figs. 4–6 are typical of what is seen throughout the analysis region mapped in Fig. 3.

B. Differential Flux

The differential fluxes computed from the multi-channel spectral inversion algorithms used to estimate the EW ratios can be compared directly to predictions from standard radiation belt models. This is done in Fig. 7 for the differential flux at 40 MeV as a function of altitude at −18 degrees longitude and 300 degrees latitude. CEASE results corresponding to the two characteristic look angles in each bin are plotted squares (circles) for the angle measuring eastward (westward) traveling particles. Uncertainty in the flux values due to the spectral fitting process and the angular dependence of the CEASE response (Fig. 1) when possibly looking at a narrowly peaked distribution toward the edge of the field of view have been estimated and are shown as error bars. Predictions from the AP-8 [8], CRRESPRO [17] and TPM-1 [18] models are shown as solid, dotted and dashed curves, respectively. Dark (light) curves for each color display the range of solar cycle variability captured by the models and represent AP8 min (max), CRRESPRO Quiet (Active) and TPM-1 with F10.7 = 95 (F10.7 = 173). [For those reading a color version of this paper the light curves for a given model are in green.] The step-like nature of the CRRESPRO curves represents the coarse resolution of the magnetic coordinates used in the model when mapped to LEO altitudes.

Measured flux values from CEASE are substantially higher the AP8 predictions and slightly above the TPM-1 and CRRESPRO predictions at higher altitudes. The best agreement comes from TPM-1. Only several profile comparisons have been constructed to date and in all cases the measurements are substantially higher than the AP8 model. Values arecloser to the other two models, and sometimes smaller in magnitude, especially at lower altitudes.

V. Conclusion

Measurements of the anisotropy of total dose and energetic proton flux have been made over a broad region of the SAA at altitudes from 400–1700 km and have compared favorably to predictions of the Lencheck and Singer [1]. The effect is not apparent above 1200 km and starts increasing rapidly below 1000 km with the rate of increase depending on location in the anomaly. For the purposes of spacecraft design it appears that use of the Lencheck and Singer formula ((1)) is sufficient to estimate the magnitude of directional effects, albeit perhaps using several density scale height curves to span the range of neutral density variation likely to be encountered. Preliminary comparisons of the magnitude of the 40 MeV differential flux to predictions from the AP8, CRRESPRO and TPM-1 models indicate that TPM-1 gives the best agreement; the data values always exceed the AP8 prediction.

Future work will focus on improving the geometric factor and spectral inversion algorithms so as to better resolve pitch angle distributions which peak well off the CEASE look angle, thereby increasing the area of the SAA which can be accurately investigated by these techniques. A more comprehensive comparison of the differential flux measurements to the models at different locations and different energies is also warranted.

Acknowledgment

The authors would like to thank S. Easley for performing preliminary analysis of the EW effect as seen by CEASE. They also thank M. Golightly and A. Ling for discussions and a helping hand. The first author, G. P. Ginet, thanks F. Marcos for discussions concerning neutral density variations and for supplying tables of the Jacchia 1977 model.

References

[1] A. M. Lenchek and S. F. Singer, "Effects of the finite gyroradii of geomagnetically trapper protons," *J. Geophys. Res.*, vol. 67, pp. 4073–4075, 1962.

[2] H. H. Heckman and G. H. Nakano, "East-West asymmetry in the flux of mirroring geomagnetically trapped protons," *J. Geophys. Res.*, vol. 68, pp. 2117–2120, 1963.

[3] H. H. Heckman and G. H. Nakano, "Low-altitude trapped protons during solar minimum period," *J. Geophys. Res.*, vol. 74, pp. 3575–3590, 1969.

[4] T. Sakaguchi, T. Doke, N. Hasebe, J. Kikuchi, S. Kono, T. Takagi, K. Takahasi, S. Nagaoka, T. Nakano, S. Takahashi, and G. D. Badhwar, "Measurement of the directional distribution of incident particles in the Shuttle-Mir mission orbit," *J. Geophys. Res.*, vol. 104, pp. 22733–22793, 1999.

[5] G. D. Badhwar, V. V. Kushin, Y. A. Akatov, and V. A. Myltseva, "Effects of trapped proton flux anisotropy on dose rates in low Earth orbit," *Radiat. Meas.*, vol. 30, pp. 415–426, 1999.

[6] P. Bühler, A. Zehnder, M. Kruglanski, E. Daly, and L. Adams, "The high-energy proton fluxes in the SAA observed with REM aboard the MIR orbital station," *Radiat. Meas.*, vol. 35, pp. 489–497, 2002.

[7] J. W. Watts, T. A. Parnell, and H. H. Heckman, "Approximate angular distribution and spectra for geomagnetically trapped protons in low-earth orbit," in *Proc. Conf. High-Energy Radiation Back-Ground Space*, A. C. Rester, Jr. and J. I. Trombka, Eds., Santibel Island, FL, 1987, pp. 75–85.

[8] D. M. Sawyer and J. I. Vette, "AP-8 trapped proton environment for solar maximum and solar minimum," NSSDC/WDC-A-R&S 76-06, Nat. Space Sci. Data Center, Goddard Spaceflight Cent.. Greenbelt, MD, 1976.

[9] T. W. Armstrong, B. L. Colborn, and J. W. Watts, "Characteristics of trapped proton anisotropy at space station altitudes," SAIC Rep. SAIC-90/1474, 1990.

[10] M. Kruglanski, "Engineering tool for trapped proton flux anisotropy evaluation," *Radiat. Meas.*, vol. 26, pp. 953–958, 1996.

[11] G. D. Badhwar and A. Konradi, "Conversion of omnidirectional proton fluxes into a pitch angle distribution," *J. Spacecraft Rockets*, vol. 27, pp. 350–352, 1990.

[12] B. K. Dichter, J. O. McGarity, M. R. Oberhardt, V. T. Jordanov, D. J. Sperry, A. C. Huber, J. A. Pantazis, E. G. Mullen, G. Ginet, and M. S. Gussenhoven, "Compact Environmental Anomaly Sensor (CEASE): A novel spacecraft instrument for in situ measurement of environmental conditions," *IEEE Trans. Nucl. Sci.*, vol. 45, no. 6, pp. 2758–2764, Dec. 1998.

[13] D. Brautigam, "Compact Environment Anomaly Sensor (CEASE): Response functions," Hanscom AFB, MA, Air Force Research Lab.Tech. Rep. AFRL-VS-HA-TR-2006-1030, 2006.

[14] D. Brautigam, Compact Environment Anomaly Sensor (CEASE): Geometric Factors in preparation.

[15] G. P. Ginet, D. Madden, B. K. Dichter, and D. H. Brautigam, "Energetic proton maps for the South Atlantic anomaly," in *Proc. IEEE Radiation Effects Data Workshop Rec.*, 2007, pp. 1–8 [Online]. Available: http://www.ieee.org/conferencepublishing

[16] L. G. Jacchia, "Thermospheric temperature, density, and composition: New models," Smithsonian Inst. Astrophysical Observatory, Cambridge, MA, Smithsonian Astrophysical Observatory Special Rep. No. 375, 1977.

[17] J. D. Meffert and M. S. Gussenhoven, "CRRESPRO Documentation," Rep. no. PL-TR-94-2218, Phillips Lab., Hanscom AFB, MA, 01731.

[18] S. L. Huston, "Space environment and effects: Trapped proton model," NASA/CR-2002-211784, NASA Marshall Spaceflight Center. Huntsvill, AL, 2002.